1 **High secondary formation of nitrogen-containing organics (NOCs) and its**

2 **possible link to oxidized organics and ammonium**

3 Guohua Zhang[1], Xiufeng Lian[1,2], Yuzhen Fu[1,2], Qinhao Lin[1], Lei Li[3], Wei Song[1], Zhanyong

4 Wang[4], Mingjin Tang[1], Duohong Chen[5], Xinhui Bi[1,*], Xinming Wang[1], Guoying Sheng[1]

5

6 [1] State Key Laboratory of Organic Geochemistry and Guangdong Key Laboratory of

7 Environmental Resources Utilization and Protection, Guangzhou Institute of Geochemistry,

8 Chinese Academy of Sciences, Guangzhou 510640, PR China

9 [2] University of Chinese Academy of Sciences, Beijing 100039, PR China

10 [3] Institute of Mass Spectrometer and Atmospheric Environment, Jinan University, Guangzhou

11 510632, PR China

12 [4] School of Intelligent Systems Engineering, Sun Yat-sen University, Shenzhen 518107, PR

13 China

14 [5] State Environmental Protection Key Laboratory of Regional Air Quality Monitoring,

15 Guangdong Environmental Monitoring Center, Guangzhou 510308, PR China

16

17 Correspondence to: Xinhui Bi (bixh@gig.ac.cn)

18

19 **Highlights**

20 ● Nitrogen-containing organics (NOCs) were highly internally mixed with photochemically

21 produced secondary oxidized organics

22 ● More than 50% of NOCs were well predicted by secondary formation from these

23 oxidized organics and ammonium

24 ● Higher relative humidity and particle acidity facilitated the formation of NOCs

Atmospheric
Chemistry
and Physics
Discussions

25   **Abstract**

26   Nitrogen-containing organic compounds (NOCs) substantially contribute to light

27   absorbing organic aerosols, although the atmospheric processes responsible for the secondary

28   formation of these compounds are poorly understood. In this study, seasonal atmospheric

29   processing of NOCs were investigated by single particle mass spectrometry in urban

30   Guangzhou from 2013-2014. The relative abundance of NOCs was found to be strongly

31   enhanced by internal mixing with the photochemically produced secondary oxidized organics

32   (such as formate, acetate, pyruvate, methylglyoxal, glyoxylate, oxalate, malonate and

33   succinate). Furthermore, the co-occurrence of NOCs with ammonium was also observed.

34   Interestingly, the relative abundance of NOCs was inversely correlated with ammonium, while

35   their number fractions were positively correlated. Multiple linear regression analysis and

36   positive matrix factorization analysis were performed to predict the relative abundance of NOCs

37   generated from oxidized organics and ammonium. Both results showed close associations ($R^2 >$

38   0.7, $p < 0.01$) between the predicted NOCs and the observed values. Increased humidity and

39   higher particle acidity were found to promote the production of NOCs. Higher relative

40   contributions of NOCs were observed in summer and autumn, in comparison to spring and

41   winter, due to the relatively higher contribution of oxidized organics and NH_3/NH_4^+ in summer

42   and autumn periods. To the best of our knowledge, this is the first direct field observation study

43   establishing a close association between NOCs and both oxidized organics and ammonium.

44   These findings have substantial implications on the role of ammonium in the atmosphere,

45   particularly in models predicting the evolution and deposition of NOCs.

46

47 **Keywords**: nitrogen-containing organic compounds, individual particles, oxidized organics,

48 ammonium, mixing state, single particle mass spectrometry

49

1 Introduction

51   Organic aerosols that strongly absorb solar radiation are referred to as brown carbon

52 (BrC), capable of a comparable level of light absorption in the spectral range of near-

53 ultraviolet (UV) light as black carbon (Andreae and Gelencser, 2006; Feng et al., 2013; Yan

54 et al., 2018). Nitrogen-containing organic compounds (NOCs) represent a large and

55 complicate fraction of atmospheric aerosols, significantly contributing to the pool of BrC

56 (Feng et al., 2013; Mohr et al., 2013; Li et al., 2019). Furthermore, NOCs have a major effect

57 on atmospheric chemistry, human health and climate forcing (Noziere et al., 2015;

58 Kanakidou et al., 2005; Shrivastava et al., 2017; De Gouw and Jimenez, 2009). The nitrogen

59 component of NOCs accounts for a large fraction of total airborne nitrogen (~30%), although

60 the proportion exhibits a high level of variability temporally and spatially and therefore has

61 an influence on both regional and global N deposition (Neff et al., 2002; Shi et al., 2010;

62 Cape et al., 2011). However, the sources, evolution and optical properties of NOCs remain

63 unclear and contribute significantly to uncertainties in the estimation of their impacts on the

64 environment and climate (Laskin et al., 2015; Feng et al., 2013).

65   NOCs are ubiquitous components of atmospheric aerosols, cloud water and rainwater

66 (Altieri et al., 2009; Desyaterik et al., 2013; Laskin et al., 2015), spanning a wide range of

67 molecular weights, structures and light absorption properties (Lin et al., 2016). Emissions of

68 primary NOCs have been attributed to biomass burning, coal combustion, vehicle emissions,

69 biogenic production and soil dust (Laskin et al., 2009; Desyaterik et al., 2013; Sun et al.,

Atmospheric
Chemistry
and Physics
Discussions
Open Access
EGU

70   2017; Mace et al., 2003; Rastogi et al., 2011; Wang et al., 2017). Growing evidence from

71   laboratory studies suggest that the production pathways for secondary NOCs in gas phase,

72   aerosol, and clouds. Maillard reactions involving mixtures of atmospheric aldehydes (e.g.,

73   methylglyoxal/glyoxal) and ammonium/amines are of particular interests (e.g., Hawkins et

74   al., 2016; De Haan et al., 2017; De Haan et al., 2011). Similarly, a significant portion of

75   NOCs may also be derived from the heterogeneous ageing of secondary organic aerosol

76   (SOA) with NH_3 / NH_4^+ (Liu et al., 2015; Laskin et al., 2015). Mang et al. (2008) proposed

77   that even trace levels of ammonia may be sufficient to form NOCs via this pathway. In

78   addition, gas phase formation of NOCs through interaction between volatile organic

79   hydrocarbons and NO_x and other oxidations, followed by condensation may also have

80   potential contribution (Fry et al., 2014; Stefenelli et al., 2019; Lehtipalo et al., 2018).

81   The secondary formation of NOCs is especially prevalent in environments experiencing

82   high anthropogenic emissions (Yu et al., 2017; Ho et al., 2015), although further studies are

83   required to comprehensively establish the formation mechanisms. A major obstacle is that

84   organic and inorganic matrix effects have a profound impact on the chemistry of organic

85   compounds in bulk aqueous particles and particles undergoing drying (El-Sayed et al., 2015;

86   Lee et al., 2013). While real-time characterization studies remain a challenge due to the

87   extremely complex chemical nature of NOCs, establishing this data along with the co-

88   variation of NOCs with other chemical components would help to identify the sources and

89   evolution of NOCs. Using single-particle aerosol time-of-flight mass spectrometry, Wang et

90   al. (2010) observed that the widespread occurrence of NOCs was closely correlated with

Atmospheric
Chemistry
and Physics
Discussions

91 particle acidity in the atmosphere of Shanghai (China). In addition, real-time measurements

92 of the atmosphere in New York (US) by aerosol mass spectrometry, indicated a positive link

93 between the age of organic species and the N/C ratio (Sun et al., 2011). Further in-depth

94 studies are required to identify the role of formation conditions (e.g., relative humidity (RH)

95 and pH) for secondary NOCs (Aiona et al., 2017; Nguyen et al., 2012). In present study, the

96 mixing state of individual particles were investigated, involving NOCs, oxidized organics

97 and ammonium, based on in-line seasonal observations using single particle aerosol mass

98 spectrometry (SPAMS). These findings show that the formation of NOCs was significantly

99 linked to oxidized organics and NH_4^+, which ought to have important environmental

100 implications for the impact and fate of these compounds.

101

102 **2 Methods**

103 **2.1 Field measurements**

104   Sampling was performed at the Guangzhou Institute of Geochemistry, a representative

105 urban site in Guangzhou (China), a megacity in the Pearl River Delta (PRD) region. SPAMS

106 analysis was performed (Hexin Analytical Instrument Co., Ltd., China) to establish the size

107 and chemical composition of individual particles in real-time (Li et al., 2011). The sampling

108 inlet for aerosol characterization was situated 40 meters above the ground level. A brief

109 description of the performance of SPAMS and other instruments can be found in the

110 Supporting Information. The sampling periods covered four seasons including spring (21/02

111 to 11/04 2014), summer (13/06 to 16/07 2013), autumn (26/09 to 19/10 2013) and winter

Atmospheric
Chemistry
and Physics
Discussions

112   (15/12 to 25/12 2013). The total measured particle numbers and mean values for

113   meteorological data and gaseous pollutants, are outlined for each season in Table S1 and

114   were described in a previous publication (Zhang et al., 2019).

115

116   **2.2 SPAMS data analysis**

117   Fragments of NOCs were identified according to detection of ion peaks at m/z -26 $[CN]^-$

118   or -42 $[CNO]^-$, generally due to the presence of C-N bonds (Silva and Prather, 2000;

119   Zawadowicz et al., 2017; Pagels et al., 2013). Thus, the NOCs herein may refer to complex

120   nitrated organics such as organic nitrates, nitro-aromatics, nitrogen heterocycles and

121   polyphenols. The bulk solution-phase reaction between the representative oxidized organics

122   (i.e., methylglyoxal) and ammonium sulfate was also performed in the laboratory to confirm

123   that the formation of C-N bonds would generate ion peaks at m/z -26 $[CN]^-$ and/or -42

124    $[CNO]^-$ using SPAMS (Fig. S1). The number fractions (Nfs) of particles that contained

125   NOCs ranged from 56-59% across all four seasons (Table S1). The number of detected

126   NOCs-containing particles and their vacuum aerodynamic diameter (d_{va}) are shown in Fig.

127   S2. Most of the detected NOC-containing particles had a d_{va} in a range of 300-1200 nm.

128   A representative mass spectrum for NOCs-containing particles is shown in Fig. 1.

129   Dominant peaks in the mass spectrum were 39 $[K]^+$, 23 $[Na]^+$, nitrate (-62 $[NO_3]^-$ or -46

130    $[NO_2]^-$), sulfate (-97 $[HSO_4]^-$), organics (27 $[C_2H_3]^+$, 63 $[C_5H_3]^+$, -42 $[CNO]^-$, -26 $[CN]^-$),

131   ammonium (18 $[NH_4]^+$) and carbon ion clusters ($C_n^{+/-}$, n = 1, 2, 3,…). NOCs-containing

132   particles were internally mixed with various oxidized organics, represented as formate at m/z

133   -45 [HCO_2]$^-$, acetate at m/z -59 [CH_3CO_2]$^-$, methylglyoxal at m/z -71 [$C_3H_3O_2$]$^-$, glyoxylate

134   at m/z -73 [C_2HO_3]$^-$, pyruvate at m/z -87 [$C_3H_3O_3$]$^-$, malonate at m/z -103 [$C_3H_3O_4$]$^-$ and

135   succinate at m/z -117 [$C_4H_5O_4$]$^-$ (Zhang et al., 2017; Zauscher et al., 2013; Lee et al., 2003).

136   The contribution of these ion peaks to the formation of secondary oxidized organics has been

137   previously confirmed based on their pronounced diurnal trends, with maximum

138   concentrations observed in the afternoon (Zhang et al., 2019). Furthermore, these oxidized

139   organics have been reported to be highly correlated (r = 0.72 - 0.94, $p < 0.01$) with each other

140   (Zhang et al., 2019), consistent with the assumption that they are photochemical oxidation

141   products of various volatile organic compounds (VOCs) (Paulot et al., 2011; Zhao et al.,

142   2012; Ho et al., 2011). More information on the seasonal variation range of the Nfs of

143   oxidized organics, ammonium and NOCs can be found in Fig. S3.

144   Hourly mean Nfs and relative peak areas were applied herein to indicate the variations

145   of aerosol compositions in individual particles. Even though advances have been made in

146   the quantification of specific chemical species for individual particles based on their

147   respective peak area information, it is still quite a challenge for SPAMS to provide

148   quantitative information on aerosol components due to matrix effects, incomplete ionization

149   and so on (Qin et al., 2006; Jeong et al., 2011; Healy et al., 2013; Zhou et al., 2016). Despite

150   of this, the variation of relative peak area should be a good indicator for the investigation of

151   atmospheric processing of various species in individual particles (Wang et al., 2010;

152   Zauscher et al., 2013; Sullivan and Prather, 2007; Zhang et al., 2014).

153

154 **3 Results and Discussion**

155 **3.1 Evidence for the formation of NOCs from oxidized organics and ammonium**

156 Figure 2 shows the seasonal variations in Nfs of the oxidized organics and ammonium,

157 which were internally mixed with NOCs. On average, more than 90% of the oxidized

158 organics and 65% of ammonium (except spring) were found to be internally mixed with

159 NOCs (Fig. S4). Based on the comparison of the Nfs of NOCs (~60%) relative to all the

160 measured particles, it may be concluded that NOCs were enhanced with the presence of

161 oxidized organics and ammonium, with the increase associated with oxidized organics being

162 most pronounced. A strong correlation between NOCs and oxidized organics further

163 demonstrates a close association between these factors, as shown in Fig. 3. Thus, the

164 dominant association between oxidized organics and NOCs (Fig. 2) indicates that NOCs

165 may be formed from the processing of secondary oxidized organics in particle phase, rather

166 than gas phase reactions followed by condensation. Water soluble organic nitrogen (WSON)

167 was reported to be positively correlated with some oxidation products in a forest in northern

168 Japan (Miyazaki et al., 2014). A close correlation observed ($R^2 = 0.55$, $p < 0.01$) between

169 the temporal variation of NOCs internally and externally mixed with oxidized organics,

170 further indicates that NOCs-containing particles free of oxidized organics may also be

171 associated with the processing of these compounds (Fig. S5). This is further supported by

172 the similar pattern of diurnal variation observed for NOCs and oxidized organics (Fig. S6).

173 However, a slight lag period was observed in the overnight peaks of NOCs, as compared to

174 those of the oxidized organics. This finding was consistent with previously reported results,

175   showing NOCs to have concentration maxima overnight in Beijing and Uintah (Yuan et al.,

176   2016; Zhang et al., 2015). The lower contribution of NOCs during daytime may be partly

177   explained by the lower RH, as discussed in section 3.2, in addition to photo-bleaching which

178   occurs during daytime (Zhao et al., 2015).

179   A previously reported study effectively modelled predictions of the diurnal variation in

180   secondary NOCs, produced by mixed carbonyls and ammonium (Woo et al., 2013). In the

181   present study, the Nfs of ammonium-containing particles internally mixed with NOCs,

182   varied within a wider range (~40-90%) (Fig. 2), as compared to the variation in oxidized

183   organics. The enhanced mixing of NOCs with ammonium suggests that the uptake of gas

184   phase oxidized organics and their interaction with particulate ammonium might also

185   contribute to the formation of NOCs (Gen et al., 2018; De Haan et al., 2017). However, no

186   enhancement occurred during spring and the enhancement was limited in ammonium-

187   containing particles, as compared to oxidized organics-containing particles (Fig. 2). This

188   phenomenon may be attributed to the limited oxidized organics fraction during spring (<

189   20%), in comparison to other seasons (~40%) (Fig. S3). Interestingly, the relationship

190   between NOCs and ammonium was distinctly different from the relationship between NOCs

191   and oxidized organics. A positive correlation ($R^2 = 0.50$, $p < 0.01$) was observed between

192   the hourly detected number of NOCs and ammonium. In contrast, a negative correlation (R^2

193    $= 0.55$, $p < 0.01$) was observed between the hourly average relative peak areas (RPAs) of

194   NOCs and ammonium (Fig. 3). These results imply that the controlling factors on the

195   formation of NOCs from ammonium are different from those controlling oxidized organics.

196   This may be due to the fact that the ammonium available to react with secondary oxidized

197   organics was from the uptake of ammonia, regarding that NOCs were mainly supplied by

198   heterogeneous reactions of oxidized organics, as discussed above. By this pathway, the

199   formation of ammonium and NOCs would compete for ammonia, potentially resulting in a

200   negative correlation between the RPAs of NOCs and ammonium as observed (Fig. 3). A

201   study shows that ammonia is more efficient at producing NOC than ammonium (Nguyen et

202   al., 2012). The negative correlation between concentrations of WSON and NH_4^+ in filter

203   samples (Fig. S7), may serve as quantitative support for the close association between

204   WSON formation and NH_4^+. Furthermore, the negative correlation between the RPA of

205   NOCs and ammonium, may indicate that the formation of NOCs is influenced by particle

206   acidity, which is directly affected by the abundance of ammonium (as discussed in section

207   3.3). Consistently, the Nfs of ammonium that internally mixed with NOCs were inversely

208   correlated with the RPAs of ammonium (Fig. S8).

209   As discussed, the formation of oxidized organics is mainly attributed to gas-phase

210   photochemical reactions followed by condensation. One may expect that NOCs were formed

211   through the interaction between NOx and oxidized organics in gas phase followed by

212   condensation (Fry et al., 2014; Stefenelli et al., 2019; Lehtipalo et al., 2018). However, low

213   correlation coefficients (R^2 = 0.02-0.13) between NOCs and NOx indicates limited

214   contribution of this pathways to the observed NOCs. Also, NOCs formed through NOx and

215   oxidized organics followed by partitioning would not be dependent on the amount of

216   ammonium, which is incompatible with our results.

217   Multiple linear regression analysis was performed to predict the RPAs of NOCs

218   generated from oxidized organics and ammonium, showing a close association ($R^2 = 0.71$,

219    $p < 0.01$) between the predicted RPAs and the observed values of NOCs (Fig. 4). Therefore,

220   the interactions involving oxidized organics and ammonium may explain over half of the

221   observed variations in NOCs in the atmosphere of Guangzhou. A fraction of the unaccounted

222   NOCs could be due to primary emissions and other formation pathways. Consistent results

223   were also obtained from the PMF model analysis (Norris et al., 2009) (detailed information

224   is provided in the SI). Fig. 5 presents the PMF factor profiles and their diurnal variations.

225   Around 75% of NOCs could be well explained by two factors, with 33% of the modelled

226   NOCs mainly associated with ammonium and carbonaceous ion peaks (ammonium factor),

227   while 59% were mainly associated with oxidized organics (oxidized organics factor). The

228   ammonium factor showed a diurnal variation pattern peaking during early morning, which

229   is consistent with the diurnal variation in RH (Zhang et al., 2019). In addition, this factor

230   contributed to ~80% (Fig. S9) of the modelled NOCs during spring when the highest RH

231   was observed (Table S1), while the oxidized organics factor dominated in all other seasons.

232   This may indicate a potential role of aqueous pathways in the formation of NOCs,

233   particularly during spring. In contrast, the oxidized organics factor showed a pattern of

234   diurnal variation, increasing from morning hours and peaking overnight, which may

235   correspond to the photochemical production of oxidized organics and follow-up interaction

236   with condensed ammonium. This pathway may explain the slightly late peaking of NOCs

237   compared to oxidized organics, as condensation of ammonium is favorable overnight (Hu et

238   al., 2008). While there were similarities in the fractions of oxidized organics in the oxalate

239   factor and the oxidized organics factor, they only contributed to 8% of the modelled NOCs

240   in the oxalate factor, which contained ~80% of the modelled oxalate. As previously

241   discussed, these oxidized organics are also precursors for the formation of oxalate (Zhang et

242   al., 2019) and therefore, these results suggest that there were two competitive pathways for

243   the evolution of these oxidized organics. Some oxidized organics formed from

244   photochemical activities were further oxidized to oxalate, resulted in a diurnal pattern of

245   variation and concentration peaks during the afternoon (Fig. 5), while others interact with

246   ammonium to form NOCs. This However, the controlling factors for these pathways could

247   not be determined in the present study.

248   Several laboratory studies have confirmed the importance of ammonium in the

249   formation of NOCs from carbonyls in atmospheric aerosols (Sareen et al., 2010; Shapiro et

250   al., 2009; Noziere et al., 2009; Kampf et al., 2016; Galloway et al., 2009). Similarly, SOA

251   generated from a large group of biogenic and anthropogenic VOCs can be further aged by

252   NH_3/NH_4^+ (Nguyen et al., 2012; Bones et al., 2010; Updyke et al., 2012; Liu et al., 2015;

253   Huang et al., 2017). In a chamber study, the formation of NOCs were found to be enhanced

254   in a NH_3-rich environment (Chu et al., 2016). While such chemical mechanisms might be

255   complex, the initial steps generally involve reactions forming imines and amines, which can

256   further react with carbonyl SOA compounds to form more complex products (e.g.,

257   oligomers/BrC) (Laskin et al., 2015).

258

3.2 Seasonal variations in the observed NOCs

259

260   A clear seasonal variation in NOCs were also observed, with higher relative

261   contributions during summer and autumn (Figs. 3 and 4), mainly due to the variations in

262   oxidized organics and NH_3/NH_4^+. As discussed in section 3.3, particle acidity was lower

263   during spring and winter than during summer and autumn, which may contribute to the

264   observed seasonal variations. In this region, a larger contribution from secondary oxidized

265   organics is typically observed during summer and autumn (Zhou et al., 2014; Yuan et al.,

266   2018). The seasonal maximum NH_3 concentrations have also been reported during the

267   warmer seasons, corresponding to the peak emissions from agricultural activities and high

268   temperatures, while the low NH_3 concentrations observed in colder seasons may be

269   attributed to gas-to-particle conversion (Pan et al., 2018; Zheng et al., 2012). Such seasonal

270   variation in NOCs were also obtained in a model simulation, showing that the conversion of

271   NH_3 into NOCs would result in a significantly higher reduction of gas-phase NH_3 during

272   summer (67%) than winter (31%), due to the higher NH_3 and SOA concentrations present in

273   the summer (Zhu et al., 2018). Since NOCs have been commonly observed in air masses

274   affected by biomass burning (Desyaterik et al., 2013), more primary NOCs may also be

275   present during summer and autumn in the present study, due to the additional biomass

276   burning activities in these seasons (Chen et al., 2018; Zhang et al., 2013).

277   While the seasonal variations in NOCs can be adequately explained by the variations in

278   concentrations of oxidized organics and ammonium (Fig. 4), the hourly variations during

279   each season were not well explained, as indicated by the lower R^2 values (Table S2). The

280   correlation coefficients (R^2) ranged from 0.24 to 0.57 for inter-seasonal variations, although

281   all regressions were found to be significant. As shown in Fig. 3, the seasonal dependence of

282   NOCs on oxidized organics and ammonium varies, despite the correlations between NOCs

283   and oxidized organics / ammonium being significant ($p < 0.01$) over different seasons.

284   During spring, NOCs exhibited a limited dependence on oxidized organics (Fig. 3a and 3b),

285   while during summer, the hourly detected number of NOCs showed a limited dependence

286   on ammonium (Fig. 3d). These findings were consistent with the PMF results, showing that

287   the ammonium factor explained ~80% of the predicted NOCs during spring, while the

288   oxidized organics factor dominantly contributed to the predicted NOCs during warmer

289   seasons (Fig. S9). A detailed discussion of this issue is provided in the SI.

290

291   **3.3 Influence of RH and particle acidity**

292   The importance of RH on NOC RPAs and peak ratios of NOCs and oxidized organics,

293   are shown in Fig. 6. While NOCs did not show a clear dependence on RH, the ratio of NOCs

294   to oxidized organics showed a clear increase with higher RH. This finding is consistent with

295   the observations reported by Xu et al. (2017), in which the N/C ratio significantly increased

296   as a function of RH in the atmosphere of Beijing. In addition, the diurnal variations of NOCs

297   with peaks values around 20:00 were also similar to those reported by Xu et al. (2017). These

298   findings imply that aqueous-phase processing likely plays an important role in the formation

299   of NOCs. Significant changes in RH, such as during the evaporation of water droplets, have

300   been reported to facilitate the formation of NOCs via NH_3/NH_4^+ and SOA (Nguyen et al.,

301   2012). In addition, an increase in RH would improve the uptake of NH_3 and formation of

302   NH_4^+, which also contributes to the enhancement of NOCs. However, the relatively weak

303   correlation ($R^2 = 0.27$, $p < 0.01$) between the peak ratios and RH, reflect the complex

304   influence of RH on the formation of NOCs (Xu et al., 2017; Woo et al., 2013). It is noted

305   that the formation of NOCs from oxidized organics was not enhanced when RH conditions

306   were lower than 40%.

307   While particulate organics with a high N/C ratio were formed in the presence of

308   ammonium salts (Lee et al., 2013), the influence of particle acidity on the formation of NOCs

309   has not previously been thoroughly evaluated. We further analyzed the influence of particle

310   acidity on the formation of NOCs, with particle acidity represented by the relative acidity

311   ratio, defined as the sum of absolute average peak areas of nitrate (m/z -62) and sulfate (m/z

312   -97) divided by those of ammonium (m/z 18) (Denkenberger et al., 2007). Fig. 7 clearly

313   shows the dependence of NOCs on particle acidity. Similarly, ambient observations reported

314   from a forest site in Japan indicate that aerosol acidity likely plays an important role in the

315   formation of WSON via acid-catalyzed reactions in summer (Miyazaki et al., 2014).

316   Enhanced organic aerosol yields from gas-phase carbonyls in the acidic seed aerosol have

317   been attributed to the occurrence of acid-catalyzed reactions (Jang et al., 2002). Furthermore,

318   acidity could also play a significant role in the gas-to-particle partitioning of aldehydes

319   (Herrmann et al., 2015; Liggio et al., 2005; Gen et al., 2018; De Haan et al., 2018; Kroll et

320   al., 2005), although some studies have indicated that browning of some SOA occurs

321   independently within a pH range of 4−10 (Nguyen et al., 2012). Consistently higher relative

322   acidity was observed for the internally mixed ammonium and NOCs particles, as compared

323   to ammonium-containing particles without NOCs (Fig. S7). This finding was consistent with

324   the results discussed in section 3.1, indicating that particles containing a higher abundance

325   of ammonium may not facilitate the formation of NOCs. A previously reported modelled

326   simulation showed that after including the chemistry of SOA ageing with NH_3, an increase

327   in aerosol acidity would be expected due to the reduction in NH_4, resulting in more SOA

328   generated from acid-catalyzed reactions (Zhu et al., 2018). Consequently, the relative acidity

329   ratio was also included in the multiple linear regression model applied in the present study,

330   as previously discussed. However, the inclusion of relative acidity did not improve the

331   degree of fit between the observed and modeled RPAs of NOCs. This suggests that the

332   selection of the RPAs of ammonium or the relative acidity ratio in regression analysis

333   resulted in similar outcomes for the formation of NOCs as the present study, due to the

334   overlap between these variables. Sulfate might also play a role in the enhancement of

335   formation kinetics for NOCs ($R^2 = 0.13$, $p < 0.01$), as previously demonstrated in laboratory

336   simulations showing that sulfate can enhance the partitioning of some carbonyls (Lee et al.,

337   2013).

338

339   **3.4 Atmospheric implications and limitation**

340   In this study we showed that in an urban megacity area, secondary NOCs were

341   significantly contributed by the heterogeneous ageing of photochemical products with

342   NH_3/NH_4^+, providing valuable insight into SOA aging mechanisms. In particular, the effects

343   of NH_3/NH_4^+ on SOA or BrC formation remain relatively poorly understood. In the PRD

344   region, it has been shown that oxygenated organic aerosols (OOA) account for more than

345   40% the total organic mass (He et al., 2011), with high concentrations of available gaseous

346   carbonyls (Li et al., 2014). Therefore, it is expected that over half of all water soluble NOCs

347   in this region, might link to secondary processing (Yu et al., 2017). Furthermore, secondary

348   sources have been found to contribute significantly to NOCs related BrC in Nanjing, China

349   (Chen et al., 2018). The results presented herein also suggest that the production of NOCs

350   might be effectively estimated by their correlation with secondary oxidized organics and

351   ammonium. The effectiveness of correlation based estimations needs to be examined in other

352   regions before being generally applied in other environments. However, this approach may

353   provide valuable insights in investigations into NOCs using atmospheric observations. In

354   contrast, it has previously been reported that a positive correlation exists between WSON

355   and ammonium (Li et al., 2012), indicating similar anthropogenic sources. This divergence

356   could be mainly attributed to varying contributions of primary sources and secondary

357   processes to the observed NOCs. Possible future reductions in anthropogenic emissions of

358   ammonia may reduce particle NOCs. Understanding the complex interplay between

359   inorganic and organic nitrogen is an important part of assessing the global nitrogen cycling.

360   Moise et al. (2015) proposed that with high concentrations of reduced nitrogen

361   compounds, high photochemical activity and frequent changes in humidity, BrC formed via

362   NH_3/NH_4^+ and SOA may become a dominant contributor to aerosol absorption, specifically

363   in agricultural and forested areas. However, this study suggests that even in typical urban

364   areas, BrC formation via NH_3/NH_4^+ and SOA should be considered. In particular, SOA was

365   found to account for 44–71% of the organic mass in megacities across China (Huang et al.,

366   2014), with NH_3 concentrations in urban areas comparable with those from agricultural sites

367   and 2- or 3-fold those of forested areas in China (Pan et al., 2018). Additionally, the acidic

368   nature of particles in these regions would be also favorable for the formation of NOCs (Guo

369   et al., 2017; Jia et al., 2018).

370   Considering the formation of NOCs from the uptake of NH_3 onto SOA particles, Zhu

371   et al. (2018) suggested that this mechanism could have a significant impact on the

372   atmospheric concentrations of NH_3/NH_4^+ and NO_3^-. However, the uptake of carbonyl onto

373   the ammonium-containing particles was not considered. As discussed above, 33% of the

374   modelled NOCs on average could be explained by the ammonium factor, with this effect

375   most pronounced during spring (Fig. 5 and Fig. S9). Such chemistry may also result in an

376   increase in aerosol acidity due to the reduction in NH_4^+, resulting in the formation of more

377   SOA from acid-catalyzed reactions of gas-phase carbonyls (Jang et al., 2002). Given that

378   RH and particle acidity play an important role in the aqueous formation of SOA and uptake

379   of NH_3, such models should be developed to include these factors, in order to improve our

380   understanding of the impact of the discussed chemical mechanisms in atmospheric chemistry

381   and the global nitrogen cycle.

382

383   **5 Conclusions**

Atmospheric
Chemistry
and Physics
Discussions

384   This study investigated the processes contributing to the seasonal formation of NOCs,

385   involving ammonium and oxidized organics in urban Guangzhou, using single particle mass

386   spectrometry. This is the first study to provide direct field observation results to confirm that

387   the variation in NOCs correlated well and strongly enhanced internal mixing with secondary

388   oxidized organics. These findings highlight the possible formation pathway of NOCs

389   through ageing of secondary oxidized organics by NH_3/NH_4^+ in ambient urban environments.

390   A clear pattern of seasonal variation in NOCs was observed, with higher relative

391   contributions in summer and autumn as compared to spring and winter. This seasonal

392   variation was well predicted by multiple linear regression model analysis, using the relative

393   abundance of oxidized organics and ammonium as model inputs. More than 50% of NOCs

394   could be explained by the interaction between oxidized organics and ammonium. The

395   production of NOCs through such processes were facilitated by increased humidity and

396   higher particle acidity. These results extend our understanding of the mixing state and

397   atmospheric processing of particulate NOCs, as well as having important implications for

398   the accuracy of models predicting the formation, fate and impacts of NOCs in the atmosphere.

399

400   **Author contribution**

401   GHZ and XHB designed the research (with input from WS, LL, ZYW, DHC, MJT, XMW

402   and GYS), analyzed the data, and wrote the manuscript. XFL, YZF and QHL conducted air

403   sampling work and laboratory experiments under the guidance of GHZ, XHB and XMW.

404   All authors contributed to the refinement of the submitted manuscript.

Atmospheric
Chemistry
and Physics
Discussions

405

References

411 **References**

412 Aiona, P. K., Lee, H. J., Leslie, R., Lin, P., Laskin, A., Laskin, J., and Nizkorodov, S. A.:

413 Photochemistry of Products of the Aqueous Reaction of Methylglyoxal with Ammonium

414 Sulfate, Acs Earth Space Chem., 1, 522-532, doi:10.1021/acsearthspacechem.7b00075, 2017.

415 Altieri, K. E., Turpin, B. J., and Seitzinger, S. P.: Composition of Dissolved Organic

416 Nitrogen in Continental Precipitation Investigated by Ultra-High Resolution FT-ICR Mass

417 Spectrometry, Environ. Sci. Technol., 43, 6950-6955, doi:10.1021/es9007849, 2009.

418 Andreae, M. O., and Gelencser, A.: Black carbon or brown carbon? The nature of light-

419 absorbing carbonaceous aerosols, Atmos. Chem. Phys., 6, 3131-3148, 2006.

420 Bones, D. L., Henricksen, D. K., Mang, S. A., Gonsior, M., Bateman, A. P., Nguyen, T.

421 B., Cooper, W. J., and Nizkorodov, S. A.: Appearance of strong absorbers and fluorophores in

422 limonene-O-3 secondary organic aerosol due to NH4+-mediated chemical aging over long time

423 scales, J. Geophys. Res.-Atmos., 115, D05203, doi:10.1029/2009jd012864, 2010.

424 Cape, J. N., Cornell, S. E., Jickells, T. D., and Nemitz, E.: Organic nitrogen in the

425 atmosphere — Where does it come from? A review of sources and methods, Atmos. Res., 102,

426 30-48, doi:10.1016/j.atmosres.2011.07.009, 2011.

427 Chen, Y., Ge, X., Chen, H., Xie, X., Chen, Y., Wang, J., Ye, Z., Bao, M., Zhang, Y., and

428 Chen, M.: Seasonal light absorption properties of water-soluble brown carbon in atmospheric

429 fine particles in Nanjing, China, Atmos. Environ.,

430 doi:https://doi.org/10.1016/j.atmosenv.2018.06.002, 2018.

431 Chu, B. W., Zhang, X., Liu, Y. C., He, H., Sun, Y., Jiang, J. K., Li, J. H., and Hao, J. M.:

432 Synergetic formation of secondary inorganic and organic aerosol: effect of SO2 and NH3 on

433 particle formation and growth, Atmos. Chem. Phys., 16, 14219-14230, doi:10.5194/acp-16-

434 14219-2016, 2016.

435 De Gouw, J., and Jimenez, J. L.: Organic Aerosols in the Earth's Atmosphere, Environ.

436 Sci. Technol., 43, 7614-7618, doi:10.1021/Es9006004, 2009.

437 De Haan, D. O., Hawkins, L. N., Kononenko, J. A., Turley, J. J., Corrigan, A. L., Tolbert,

438 M. A., and Jimenez, J. L.: Formation of Nitrogen-Containing Oligomers by Methylglyoxal and

439   Amines in Simulated Evaporating Cloud Droplets, Environ. Sci. Technol., 45, 984-991,

440   doi:10.1021/es102933x, 2011.

441   De Haan, D. O., Hawkins, L. N., Welsh, H. G., Pednekar, R., Casar, J. R., Pennington, E.

442   A., de Loera, A., Jimenez, N. G., Symons, M. A., Zauscher, M., Pajunoja, A., Caponi, L.,

443   Cazaunau, M., Formenti, P., Gratien, A., Pangui, E., and Doussin, J.-F.: Brown Carbon

444   Production in Ammonium- or Amine-Containing Aerosol Particles by Reactive Uptake of

445   Methylglyoxal and Photolytic Cloud Cycling, Environ. Sci. Technol., 51, 7458-7466,

446   doi:10.1021/acs.est.7b00159, 2017.

447   De Haan, D. O., Jimenez, N. G., de Loera, A., Cazaunau, M., Gratien, A., Pangui, E., and

448   Doussin, J.-F.: Methylglyoxal Uptake Coefficients on Aqueous Aerosol Surfaces, J. Phys.

449   Chem. A, 122, 4854-4860, doi:10.1021/acs.jpca.8b00533, 2018.

450   Denkenberger, K. A., Moffet, R. C., Holecek, J. C., Rebotier, T. P., and Prather, K. A.:

451   Real-time, single-particle measurements of oligomers in aged ambient aerosol particles,

452   Environ. Sci. Technol., 41, 5439-5446, doi:10.1021/es070329l, 2007.

453   Desyaterik, Y., Sun, Y., Shen, X., Lee, T., Wang, X., Wang, T., and Collett, J. L., Jr.:

454   Speciation of "brown" carbon in cloud water impacted by agricultural biomass burning in

455   eastern China, J. Geophys. Res.-Atmos., 118, 7389-7399, doi:10.1002/jgrd.50561, 2013.

456   El-Sayed, M. M. H., Wang, Y. Q., and Hennigan, C. J.: Direct atmospheric evidence for

457   the irreversible formation of aqueous secondary organic aerosol, Geophys. Res. Lett., 42, 5577-

458   5586, doi:10.1002/2015gl064556, 2015.

459   Feng, Y., Ramanathan, V., and Kotamarthi, V. R.: Brown carbon: a significant

460   atmospheric absorber of solar radiation?, Atmos. Chem. Phys., 13, 8607-8621,

461   doi:10.5194/acp-13-8607-2013, 2013.

462   Fry, J. L., Draper, D. C., Barsanti, K. C., Smith, J. N., Ortega, J., Winkle, P. M., Lawler,

463   M. J., Brown, S. S., Edwards, P. M., Cohen, R. C., and Lee, L.: Secondary Organic Aerosol

464   Formation and Organic Nitrate Yield from NO3 Oxidation of Biogenic Hydrocarbons, Environ.

465   Sci. Technol., 48, 11944-11953, doi:10.1021/es502204x, 2014.

466   Galloway, M. M., Chhabra, P. S., Chan, A. W. H., Surratt, J. D., Flagan, R. C., Seinfeld,

467   J. H., and Keutsch, F. N.: Glyoxal uptake on ammonium sulphate seed aerosol: reaction

468   products and reversibility of uptake under dark and irradiated conditions, Atmos. Chem. Phys.,

469   9, 3331-3345, doi:10.5194/acp-9-3331-2009, 2009.

470   Gen, M., Huang, D. D., and Chan, C. K.: Reactive Uptake of Glyoxal by Ammonium-

471   Containing Salt Particles as a Function of Relative Humidity, Environ. Sci. Technol., 52, 6903-

472   6911, doi:10.1021/acs.est.8b00606, 2018.

473   Guo, H., Weber, R. J., and Nenes, A.: High levels of ammonia do not raise fine particle

474   pH sufficiently to yield nitrogen oxide-dominated sulfate production, Sci. Rep., 7, 12109,

475   doi:10.1038/s41598-017-11704-0, 2017.

476   Hawkins, L. N., Lemire, A. N., Galloway, M. M., Corrigan, A. L., Turley, J. J., Espelien,

477   B. M., and De Haan, D. O.: Maillard Chemistry in Clouds and Aqueous Aerosol As a Source

478   of Atmospheric Humic-Like Substances, Environ. Sci. Technol., 50, 7443-7452,

479   doi:10.1021/acs.est.6b00909, 2016.

480   He, L. Y., Huang, X. F., Xue, L., Hu, M., Lin, Y., Zheng, J., Zhang, R. Y., and Zhang, Y.

481   H.: Submicron aerosol analysis and organic source apportionment in an urban atmosphere in

482   Pearl River Delta of China using high-resolution aerosol mass spectrometry, J. Geophys. Res.-

483   Atmos., 116, 1-15, doi:10.1029/2010jd014566, 2011.

484   Healy, R. M., Sciare, J., Poulain, L., Crippa, M., Wiedensohler, A., Prevot, A. S. H.,

485   Baltensperger, U., Sarda-Esteve, R., McGuire, M. L., Jeong, C. H., McGillicuddy, E., O'Connor,

486   I. P., Sodeau, J. R., Evans, G. J., and Wenger, J. C.: Quantitative determination of carbonaceous

487   particle mixing state in Paris using single-particle mass spectrometer and aerosol mass

488   spectrometer measurements, Atmos. Chem. Phys., 13, 9479-9496, doi:10.5194/acp-13-9479-

489   2013, 2013.

490   Herrmann, H., Schaefer, T., Tilgner, A., Styler, S. A., Weller, C., Teich, M., and Otto, T.:

491   Tropospheric Aqueous-Phase Chemistry: Kinetics, Mechanisms, and Its Coupling to a

492   Changing Gas Phase, Chem. Rev., 115, 4259-4334, doi:10.1021/cr500447k, 2015.

493   Ho, K. F., Ho, S. S. H., Lee, S. C., Kawamura, K., Zou, S. C., Cao, J. J., and Xu, H. M.:

494   Summer and winter variations of dicarboxylic acids, fatty acids and benzoic acid in PM2.5 in

495   Pearl Delta River Region, China, Atmos. Chem. Phys., 11, 2197-2208, doi:10.5194/acp-11-

496   2197-2011, 2011.

497   Ho, K. F., Ho, S. S. H., Huang, R. J., Liu, S. X., Cao, J. J., Zhang, T., Chuang, H. C., Chan,

498   C. S., Hu, D., and Tian, L. W.: Characteristics of water-soluble organic nitrogen in fine

499   particulate matter in the continental area of China, Atmos. Environ., 106, 252-261,

500   doi:10.1016/j.atmosenv.2015.02.010, 2015.

501   Hu, M., Wu, Z., Slanina, J., Lin, P., Liu, S., and Zeng, L.: Acidic gases, ammonia and

502   water-soluble ions in PM2.5 at a coastal site in the Pearl River Delta, China, Atmos. Environ.,

503   42, 6310-6320, 2008.

504   Huang, M., Xu, J., Cai, S., Liu, X., Zhao, W., Hu, C., Gu, X., Fang, L., and Zhang, W.:

505   Characterization of brown carbon constituents of benzene secondary organic aerosol aged with

506   ammonia, J. Atmos. Chem., 75, 205-218, doi:10.1007/s10874-017-9372-x, 2017.

507   Huang, R. J., Zhang, Y., Bozzetti, C., Ho, K. F., Cao, J. J., Han, Y., Daellenbach, K. R.,

508   Slowik, J. G., Platt, S. M., Canonaco, F., Zotter, P., Wolf, R., Pieber, S. M., Bruns, E. A., Crippa,

509   M., Ciarelli, G., Piazzalunga, A., Schwikowski, M., Abbaszade, G., Schnelle-Kreis, J.,

510   Zimmermann, R., An, Z., Szidat, S., Baltensperger, U., El Haddad, I., and Prevot, A. S.: High

511   secondary aerosol contribution to particulate pollution during haze events in China, Nature, 514,

512   218-222, doi:10.1038/nature13774, 2014.

513   Jang, M., Czoschke, N. M., Lee, S., and Kamens, R. M.: Heterogeneous atmospheric

514   aerosol production by acid-catalyzed particle-phase reactions, Science, 298, 814-817, 2002.

515   Jeong, C. H., McGuire, M. L., Godri, K. J., Slowik, J. G., Rehbein, P. J. G., and Evans, G.

516   J.: Quantification of aerosol chemical composition using continuous single particle

517   measurements, Atmos. Chem. Phys., 11, 7027-7044, doi:10.5194/acp-11-7027-2011, 2011.

518   Jia, S. G., Sarkar, S., Zhang, Q., Wang, X. M., Wu, L. L., Chen, W. H., Huang, M. J.,

519   Zhou, S. Z., Zhang, J. P., Yuan, L., and Yang, L. M.: Characterization of diurnal variations of

520   PM2.5 acidity using an open thermodynamic system: A case study of Guangzhou, China,

521   Chemosphere, 202, 677-685, doi:10.1016/j.chemosphere.2018.03.127, 2018.

522   Kampf, C. J., Filippi, A., Zuth, C., Hoffmann, T., and Opatz, T.: Secondary brown carbon

523   formation via the dicarbonyl imine pathway: nitrogen heterocycle formation and synergistic

524   effects, Phys. Chem. Chem. Phys., 18, 18353-18364, doi:10.1039/c6cp03029g, 2016.

525   Kanakidou, M., Seinfeld, J. H., Pandis, S. N., Barnes, I., Dentener, F. J., Facchini, M. C.,

526   Van Dingenen, R., Ervens, B., Nenes, A., Nielsen, C. J., Swietlicki, E., Putaud, J. P., Balkanski,

527   Y., Fuzzi, S., Horth, J., Moortgat, G. K., Winterhalter, R., Myhre, C. E. L., Tsigaridis, K.,

528   Vignati, E., Stephanou, E. G., and Wilson, J.: Organic aerosol and global climate modelling: a

529   review, Atmos. Chem. Phys., 5, 1053-1123, 2005.

530   Kroll, J. H., Ng, N. L., Murphy, S. M., Varutbangkul, V., Flagan, R. C., and Seinfeld, J.

531   H.: Chamber studies of secondary organic aerosol growth by reactive uptake of simple carbonyl

532   compounds, J. Geophys. Res.-Atmos., 110, doi:10.1029/2005JD006004, 2005.

533   Laskin, A., Smith, J. S., and Laskin, J.: Molecular Characterization of Nitrogen-

534   Containing Organic Compounds in Biomass Burning Aerosols Using High-Resolution Mass

535   Spectrometry, Environ. Sci. Technol., 43, 3764-3771, doi:10.1021/es803456n, 2009.

536   Laskin, A., Laskin, J., and Nizkorodov, S. A.: Chemistry of Atmospheric Brown Carbon,

537   Chem. Rev., 115, 4335-4382, doi:10.1021/cr5006167, 2015.

538   Lee, A. K. Y., Zhao, R., Li, R., Liggio, J., Li, S. M., and Abbatt, J. P. D.: Formation of

539   Light Absorbing Organo-Nitrogen Species from Evaporation of Droplets Containing Glyoxal

540   and Ammonium Sulfate, Environ. Sci. Technol., 47, 12819-12826, doi:10.1021/es402687w,

541   2013.

542   Lee, S. H., Murphy, D. M., Thomson, D. S., and Middlebrook, A. M.: Nitrate and oxidized

543   organic ions in single particle mass spectra during the 1999 Atlanta Supersite Project, J.

544   Geophys. Res., 108, 8417, doi:10.1029/2001jd001455, 2003.

545   Lehtipalo, K., Yan, C., Dada, L., Bianchi, F., Xiao, M., Wagner, R., Stolzenburg, D.,

546   Ahonen, L. R., Amorim, A., Baccarini, A., Bauer, P. S., Baumgartner, B., Bergen, A.,

547   Bernhammer, A.-K., Breitenlechner, M., Brilke, S., Buchholz, A., Mazon, S. B., Chen, D., Chen,

548 X., Dias, A., Dommen, J., Draper, D. C., Duplissy, J., Ehn, M., Finkenzeller, H., Fischer, L.,

549 Frege, C., Fuchs, C., Garmash, O., Gordon, H., Hakala, J., He, X., Heikkinen, L., Heinritzi, M.,

550 Helm, J. C., Hofbauer, V., Hoyle, C. R., Jokinen, T., Kangasluoma, J., Kerminen, V.-M., Kim,

551 C., Kirkby, J., Kontkanen, J., Kürten, A., Lawler, M. J., Mai, H., Mathot, S., Mauldin, R. L.,

552 Molteni, U., Nichman, L., Nie, W., Nieminen, T., Ojdanic, A., Onnela, A., Passananti, M.,

553 Petäjä, T., Piel, F., Pospisilova, V., Quéléver, L. L. J., Rissanen, M. P., Rose, C., Sarnela, N.,

554 Schallhart, S., Schuchmann, S., Sengupta, K., Simon, M., Sipilä, M., Tauber, C., Tomé, A.,

555 Tröstl, J., Väisänen, O., Vogel, A. L., Volkamer, R., Wagner, A. C., Wang, M., Weitz, L.,

556 Wimmer, D., Ye, P., Ylisirniö, A., Zha, Q., Carslaw, K. S., Curtius, J., Donahue, N. M., Flagan,

557 R. C., Hansel, A., Riipinen, I., Virtanen, A., Winkler, P. M., Baltensperger, U., Kulmala, M.,

558 and Worsnop, D. R.: Multicomponent new particle formation from sulfuric acid, ammonia, and

559 biogenic vapors, Sci. Adv., 4, eaau5363, doi:10.1126/sciadv.aau5363, 2018.

560 Li, J., Fang, Y. T., Yoh, M., Wang, X. M., Wu, Z. Y., Kuang, Y. W., and Wen, D. Z.:

561 Organic nitrogen deposition in precipitation in metropolitan Guangzhou city of southern China,

562 Atmos. Res., 113, 57-67, doi:10.1016/j.atmosres.2012.04.019, 2012.

563 Li, L., Huang, Z. X., Dong, J. G., Li, M., Gao, W., Nian, H. Q., Fu, Z., Zhang, G. H., Bi,

564 X. H., Cheng, P., and Zhou, Z.: Real time bipolar time-of-flight mass spectrometer for analyzing

565 single aerosol particles, Intl. J. Mass. Spectrom., 303, 118-124, doi:10.1016/j.ijms.2011.01.017,

566 2011.

567 Li, X., Rohrer, F., Brauers, T., Hofzumahaus, A., Lu, K., Shao, M., Zhang, Y. H., and

568 Wahner, A.: Modeling of HCHO and CHOCHO at a semi-rural site in southern China during

569 the PRIDE-PRD2006 campaign, Atmos. Chem. Phys., 14, 12291-12305, doi:10.5194/acp-14-

570 12291-2014, 2014.

571 Li, Z. J., Nizkorodov, S. A., Chen, H., Lu, X. H., Yang, X., and Chen, J. M.: Nitrogen-

572 containing secondary organic aerosol formation by acrolein reaction with ammonia/ammonium,

573 Atmos. Chem. Phys., 19, 1343-1356, doi:10.5194/acp-19-1343-2019, 2019.

574 Liggio, J., Li, S. M., and Mclaren, R.: Reactive uptake of glyoxal by particulate matter, J.

575 Geophys. Res.-Atmos., 110, doi:10.1029/2004jd005113, 2005.

576   Lin, P., Aiona, P. K., Li, Y., Shiraiwa, M., Laskin, J., Nizkorodov, S. A., and Laskin, A.:

577   Molecular Characterization of Brown Carbon in Biomass Burning Aerosol Particles, Environ.

578   Sci. Technol., 50, 11815-11824, doi:10.1021/acs.est.6603024, 2016.

579   Liu, Y., Liggio, J., Staebler, R., and Li, S. M.: Reactive uptake of ammonia to secondary

580   organic aerosols: kinetics of organonitrogen formation, Atmos. Chem. Phys., 15, 13569-13584,

581   doi:10.5194/acp-15-13569-2015, 2015.

582   Mace, K. A., Kubilay, N., and Duce, R. A.: Organic nitrogen in rain and aerosol in the

583   eastern Mediterranean atmosphere: An association with atmospheric dust, J. Geophys. Res.-

584   Atmos., 108, doi:10.1029/2002jd002997, 2003.

585   Mang, S. A., Henricksen, D. K., Bateman, A. P., Andersen, M. P. S., Blake, D. R., and

586   Nizkorodov, S. A.: Contribution of Carbonyl Photochemistry to Aging of Atmospheric

587   Secondary Organic Aerosol, J. Phys. Chem. A, 112, 8337-8344, doi:10.1021/jp804376c, 2008.

588   Miyazaki, Y., Fu, P. Q., Ono, K., Tachibana, E., and Kawamura, K.: Seasonal cycles of

589   water-soluble organic nitrogen aerosols in a deciduous broadleaf forest in northern Japan, J.

590   Geophys. Res.-Atmos., 119, 1440-1454, doi:10.1002/2013JD020713, 2014.

591   Mohr, C., Lopez-Hilfiker, F. D., Zotter, P., Prévôt, A. S. H., Xu, L., Ng, N. L., Herndon,

592   S. C., Williams, L. R., Franklin, J. P., Zahniser, M. S., Worsnop, D. R., Knighton, W. B., Aiken,

593   A. C., Gorkowski, K. J., Dubey, M. K., Allan, J. D., and Thornton, J. A.: Contribution of

594   Nitrated Phenols to Wood Burning Brown Carbon Light Absorption in Detling, United

595   Kingdom during Winter Time, Environ. Sci. Technol., 47, 6316-6324, doi:10.1021/es400683v,

596   2013.

597   Moise, T., Flores, J. M., and Rudich, Y.: Optical Properties of Secondary Organic Aerosols

598   and Their Changes by Chemical Processes, Chem. Rev., 115, 4400-4439,

599   doi:10.1021/cr5005259, 2015.

600   Neff, J. C., Holland, E. A., Dentener, F. J., McDowell, W. H., and Russell, K. M.: The

601   origin, composition and rates of organic nitrogen deposition: A missing piece of the nitrogen

602   cycle?, Biogeochemistry, 57, 99-136, 2002.

603   Nguyen, T. B., Lee, P. B., Updyke, K. M., Bones, D. L., Laskin, J., Laskin, A., and

604   Nizkorodov, S. A.: Formation of nitrogen- and sulfur-containing light-absorbing compounds

605   accelerated by evaporation of water from secondary organic aerosols, J. Geophys. Res.-Atmos.,

606   117, D01207, doi:10.1029/2011jd016944, 2012.

607   Norris, G., Vedantham, R., Wade, K., Zahn, P., Brown, S., Paatero, P., Eberly, S., and

608   Foley, C. (2009), Guidance document for PMF applications with the Multilinear Engine, edited,

609   Prepared for the U.S. Environmental Protection Agency, Research Triangle Park, NC.

610   Noziere, B., Dziedzic, P., and Cordova, A.: Products and Kinetics of the Liquid-Phase

611   Reaction of Glyoxal Catalyzed by Ammonium Ions (NH4+), J. Phys. Chem. A, 113, 231-237,

612   doi:10.1021/jp8078293, 2009.

613   Noziere, B., Kaberer, M., Claeys, M., Allan, J., D'Anna, B., Decesari, S., Finessi, E.,

614   Glasius, M., Grgic, I., Hamilton, J. F., Hoffmann, T., Iinuma, Y., Jaoui, M., Kahno, A., Kampf,

615   C. J., Kourtchev, I., Maenhaut, W., Marsden, N., Saarikoski, S., Schnelle-Kreis, J., Surratt, J.

616   D., Szidat, S., Szmigielski, R., and Wisthaler, A.: The Molecular Identification of Organic

617   Compounds in the Atmosphere: State of the Art and Challenges, Chem. Rev., 115, 3919-3983,

618   doi:10.1021/cr5003485, 2015.

619   Pagels, J., Dutcher, D. D., Stolzenburg, M. R., McMurry, P. H., Galli, M. E., and Gross,

620   D. S.: Fine-particle emissions from solid biofuel combustion studied with single-particle mass

621   spectrometry: Identification of markers for organics, soot, and ash components, J. Geophys.

622   Res.-Atmos., 118, 859-870, doi:10.1029/2012jd018389, 2013.

623   Pan, Y. P., Tian, S. L., Zhao, Y. H., Zhang, L., Zhu, X. Y., Gao, J., Huang, W., Zhou, Y.

624   B., Song, Y., Zhang, Q., and Wang, Y. S.: Identifying Ammonia Hotspots in China Using a

625   National   Observation   Network,   Environ.   Sci.   Technol.,   52,   3926-3934,

626   doi:10.1021/acs.est.7b05235, 2018.

627   Paulot, F., Wunch, D., Crounse, J. D., Toon, G. C., Millet, D. B., DeCarlo, P. F.,

628   Vigouroux, C., Deutscher, N. M., González Abad, G., Notholt, J., Warneke, T., Hannigan, J.

629   W., Warneke, C., de Gouw, J. A., Dunlea, E. J., De Mazière, M., Griffith, D. W. T., Bernath,

630   P., Jimenez, J. L., and Wennberg, P. O.: Importance of secondary sources in the atmospheric

631   budgets of formic and acetic acids, Atmos. Chem. Phys., 11, 1989-2013, doi:10.5194/acp-11-

632   1989-2011, 2011.

633   Qin, X. Y., Bhave, P. V., and Prather, K. A.: Comparison of two methods for obtaining

634   quantitative mass concentrations from aerosol time-of-flight mass spectrometry measurements,

635   Anal. Chem., 78, 6169-6178, doi:10.1021/ac060395q, 2006.

636   Rastogi, N., Zhang, X., Edgerton, E. S., Ingall, E., and Weber, R. J.: Filterable water-

637   soluble organic nitrogen in fine particles over the southeastern USA during summer, Atmos.

638   Environ., 45, 6040-6047, doi:10.1016/j.atmosenv.2011.07.045, 2011.

639   Sareen, N., Schwier, A. N., Shapiro, E. L., Mitroo, D., and McNeill, V. F.: Secondary

640   organic material formed by methylglyoxal in aqueous aerosol mimics, Atmos. Chem. Phys., 10,

641   997-1016, doi:10.5194/acp-10-997-2010, 2010.

642   Shapiro, E. L., Szprengiel, J., Sareen, N., Jen, C. N., Giordano, M. R., and McNeill, V. F.:

643   Light-absorbing secondary organic material formed by glyoxal in aqueous aerosol mimics,

644   Atmos. Chem. Phys., 9, 2289-2300, 2009.

645   Shi, J., Gao, H., Qi, J., Zhang, J., and Yao, X.: Sources, compositions, and distributions of

646   water-soluble organic nitrogen in aerosols over the China Sea, J. Geophys. Res.-Atmos., 115,

647   doi:10.1029/2009jd013238, 2010.

648   Shrivastava, M., Cappa, C. D., Fan, J. W., Goldstein, A. H., Guenther, A. B., Jimenez, J.

649   L., Kuang, C., Laskin, A., Martin, S. T., Ng, N. L., Petaja, T., Pierce, J. R., Rasch, P. J., Roldin,

650   P., Seinfeld, J. H., Shilling, J., Smith, J. N., Thornton, J. A., Volkamer, R., Wang, J., Worsnop,

651   D. R., Zaveri, R. A., Zelenyuk, A., and Zhang, Q.: Recent advances in understanding secondary

652   organic aerosol: Implications for global climate forcing, Rev. Geophys., 55, 509-559,

653   doi:10.1002/2016RG000540, 2017.

654   Silva, P. J., and Prather, K. A.: Interpretation of mass spectra from organic compounds in

655   aerosol time-of-flight mass spectrometry, Anal. Chem., 72, 3553-3562, 2000.

656   Stefenelli, G., Pospisilova, V., Lopez-Hilfiker, F. D., Daellenbach, K. R., Hüglin, C., Tong,

657   Y., Baltensperger, U., Prevot, A. S. H., and Slowik, J. G.: Organic aerosol source apportionment

658   in Zurich using extractive electrospray ionization time-of-flight mass spectrometry (EESI-TOF):

659   Part I, biogenic influences and day/night chemistry in summer, Atmos. Chem. Phys. Discuss.,

660   2019, 1-36, doi:10.5194/acp-2019-361, 2019.

661   Sullivan, R. C., and Prather, K. A.: Investigations of the diurnal cycle and mixing state of

662   oxalic acid in individual particles in Asian aerosol outflow, Environ. Sci. Technol., 41, 8062-

663   8069, 2007.

664   Sun, J. Z., Zhi, G. R., Hitzenberger, R., Chen, Y. J., Tian, C. G., Zhang, Y. Y., Feng, Y.

665   L., Cheng, M. M., Zhang, Y. Z., Cai, J., Chen, F., Qiu, Y., Jiang, Z., Li, J., Zhang, G., and Mo,

666   Y.: Emission factors and light absorption properties of brown carbon from household coal

667   combustion in China, Atmos. Chem. Phys., 17, 4769-4780, doi:10.5194/acp-17-4769-2017,

668   2017.

669   Sun, Y. L., Zhang, Q., Schwab, J. J., Demerjian, K. L., Chen, W. N., Bae, M. S., Hung, H.

670   M., Hogrefe, O., Frank, B., Rattigan, O. V., and Lin, Y. C.: Characterization of the sources and

671   processes of organic and inorganic aerosols in New York city with a high-resolution time-of-

672   flight aerosol mass apectrometer, Atmos. Chem. Phys., 11, 1581-1602, doi:10.5194/acp-11-

673   1581-2011, 2011.

674   Updyke, K. M., Nguyen, T. B., and Nizkorodov, S. A.: Formation of brown carbon via

675   reactions of ammonia with secondary organic aerosols from biogenic and anthropogenic

676   precursors, Atmos. Environ., 63, 22-31, doi:10.1016/j.atmosenv.2012.09.012, 2012.

677   Wang, X. F., Gao, S., Yang, X., Chen, H., Chen, J. M., Zhuang, G. S., Surratt, J. D., Chan,

678   M. N., and Seinfeld, J. H.: Evidence for High Molecular Weight Nitrogen-Containing Organic

679   Salts in Urban Aerosols, Environ. Sci. Technol., 44, 4441-4446, 2010.

680   Wang, X. F., Wang, H. L., Jing, H., Wang, W. N., Cui, W. D., Williams, B. J., and Biswas,

681   P.: Formation of Nitrogen-Containing Organic Aerosol during Combustion of High-Sulfur-

682   Content Coal, Energ. Fuel., 31, 14161-14168, doi:10.1021/acs.energyfuels.7b02273, 2017.

683   Woo, J. L., Kim, D. D., Schwier, A. N., Li, R. Z., and McNeill, V. F.: Aqueous aerosol

684   SOA formation: impact on aerosol physical properties, Faraday Discuss., 165, 357-367,

685   doi:10.1039/c3fd00032j, 2013.

Atmospheric
Chemistry
and Physics
Discussions

686   Xu, W. Q., Sun, Y. L., Wang, Q. Q., Du, W., Zhao, J., Ge, X. L., Han, T. T., Zhang, Y. J.,

687   Zhou, W., Li, J., Fu, P. Q., Wang, Z. F., and Worsnop, D. R.: Seasonal Characterization of

688   Organic Nitrogen in Atmospheric Aerosols Using High Resolution Aerosol Mass Spectrometry

689   in   Beijing,   China,   Acs   Earth   Space   Chem.,   1,   673-682,

690   doi:10.1021/acsearthspacechem.7b00106, 2017.

691   Yan, J., Wang, X., Gong, P., Wang, C., and Cong, Z.: Review of brown carbon aerosols:

692   Recent   progress   and   perspectives,   Sci.   Total.   Environ.,   634,   1475-1485,

693   doi:https://doi.org/10.1016/j.scitotenv.2018.04.083, 2018.

694   Yu, X., Yu, Q. Q., Zhu, M., Tang, M. J., Li, S., Yang, W. Q., Zhang, Y. L., Deng, W., Li,

695   G. H., Yu, Y. G., Huang, Z. H., Song, W., Ding, X., Hu, Q. H., Li, J., Bi, X. H., and Wang, X.

696   M.: Water Soluble Organic Nitrogen (WSON) in Ambient Fine Particles Over a Megacity in

697   South China: Spatiotemporal Variations and Source Apportionment, J. Geophys. Res.-Atmos.,

698   122, 13045-13060, doi:10.1002/2017JD027327, 2017.

699   Yuan, B., Liggio, J., Wentzell, J., Li, S. M., Stark, H., Roberts, J. M., Gilman, J., Lerner,

700   B., Warneke, C., Li, R., Leithead, A., Osthoff, H. D., Wild, R., Brown, S. S., and de Gouw, J.

701   A.: Secondary formation of nitrated phenols: insights from observations during the Uintah

702   BasinWinter Ozone Study (UBWOS) 2014, Atmos. Chem. Phys., 16, 2139-2153,

703   doi:10.5194/acp-16-2139-2016, 2016.

704   Yuan, Q., Lai, S., Song, J., Ding, X., Zheng, L., Wang, X., Zhao, Y., Zheng, J., Yue, D.,

705   Zhong, L., Niu, X., and Zhang, Y.: Seasonal cycles of secondary organic aerosol tracers in rural

706   Guangzhou, Southern China: The importance of atmospheric oxidants, Environ. Pollut., 240,

707   884-893, doi:10.1016/j.envpol.2018.05.009, 2018.

708   Zauscher, M. D., Wang, Y., Moore, M. J. K., Gaston, C. J., and Prather, K. A.: Air Quality

709   Impact and Physicochemical Aging of Biomass Burning Aerosols during the 2007 San Diego

710   Wildfires, Environ. Sci. Technol., 47, 7633-7643, doi:10.1021/es4004137, 2013.

711   Zawadowicz, M. A., Froyd, K. D., Murphy, D. M., and Cziczo, D. J.: Improved

712   identification of primary biological aerosol particles using single-particle mass spectrometry,

713   Atmos. Chem. Phys., 17, 7193-7212, doi:10.5194/acp-17-7193-2017, 2017.

714   Zhang, G., Lin, Q., Peng, L., Yang, Y., Jiang, F., Liu, F., Song, W., Chen, D., Cai, Z., Bi,

715   X., Miller, M., Tang, M., Huang, W., Wang, X., Peng, P., and Sheng, G.: Oxalate Formation

716   Enhanced by Fe-Containing Particles and Environmental Implications, Environ. Sci. Technol.,

717   53, 1269-1277, doi:10.1021/acs.est.8b05280, 2019.

718   Zhang, G. H., Bi, X. H., He, J. J., Chen, D. H., Chan, L. Y., Xie, G. W., Wang, X. M.,

719   Sheng, G. Y., Fu, J. M., and Zhou, Z.: Variation of secondary coatings associated with

720   elemental carbon by single particle analysis, Atmos. Environ., 92, 162-170,

721   doi:10.1016/j.atmosenv.2014.04.018, 2014.

722   Zhang, G. H., Lin, Q. H., Peng, L., Yang, Y. X., Fu, Y. Z., Bi, X. H., Li, M., Chen, D. H.,

723   Chen, J. X., Cai, Z., Wang, X. M., Peng, P. A., Sheng, G. Y., and Zhou, Z.: Insight into the in-

724   cloud formation of oxalate based on in situ measurement by single particle mass spectrometry,

725   Atmos. Chem. Phys., 17, 13891-13901, doi:10.5194/acp-17-13891-2017, 2017.

726   Zhang, Q., Duan, F., He, K., Ma, Y., Li, H., Kimoto, T., and Zheng, A.: Organic nitrogen

727   in PM2.5 in Beijing, Frontiers of Environmental Science & Engineering, 9, 1004-1014,

728   doi:10.1007/s11783-015-0799-5, 2015.

729   Zhang, Y. S., Shao, M., Lin, Y., Luan, S. J., Mao, N., Chen, W. T., and Wang, M.:

730   Emission inventory of carbonaceous pollutants from biomass burning in the Pearl River Delta

731   Region, China, Atmos. Environ., 76, 189-199, doi:10.1016/j.atmosenv.2012.05.055, 2013.

732   Zhao, R., Lee, A. K. Y., and Abbatt, J. P. D.: Investigation of Aqueous-Phase

733   Photooxidation of Glyoxal and Methylglyoxal by Aerosol Chemical Ionization Mass

734   Spectrometry: Observation of Hydroxyhydroperoxide Formation, J. Phys. Chem. A, 116, 6253-

735   6263, doi:10.1021/jp211528d, 2012.

736   Zhao, R., Lee, A. K. Y., Huang, L., Li, X., Yang, F., and Abbatt, J. P. D.: Photochemical

737   processing of aqueous atmospheric brown carbon, Atmos. Chem. Phys., 15, 6087-6100,

738   doi:10.5194/acp-15-6087-2015, 2015.

739   Zheng, J. Y., Yin, S. S., Kang, D. W., Che, W. W., and Zhong, L. J.: Development and

740   uncertainty analysis of a high-resolution NH3 emissions inventory and its implications with

741   precipitation over the Pearl River Delta region, China, Atmos. Chem. Phys., 12, 7041-7058,

742   doi:10.5194/acp-12-7041-2012, 2012.

743   Zhou, S. Z., Wang, T., Wang, Z., Li, W. J., Xu, Z., Wang, X. F., Yuan, C., Poon, C. N.,

744   Louie, P. K. K., Luk, C. W. Y., and Wang, W. X.: Photochemical evolution of organic aerosols

745   observed in urban plumes from Hong Kong and the Pearl River Delta of China, Atmos. Environ.,

746   88, 219-229, doi:10.1016/j.atmosenv.2014.01.032, 2014.

747   Zhou, Y., Huang, X. H. H., Griffith, S. M., Li, M., Li, L., Zhou, Z., Wu, C., Meng, J. W.,

748   Chan, C. K., Louie, P. K. K., and Yu, J. Z.: A field measurement based scaling approach for

749   quantification of major ions, organic carbon, and elemental carbon using a single particle

750   aerosol   mass   spectrometer,   Atmos.   Environ.,   143,   300-312,

751   doi:10.1016/j.atmosenv.2016.08.054, 2016.

752   Zhu, S. P., Horne, J. R., Montoya-Aguilera, J., Hinks, M. L., Nizkorodov, S. A., and

753   Dabdub, D.: Modeling reactive ammonia uptake by secondary organic aerosol in CMAQ:

754   application to the continental US, Atmos. Chem. Phys., 18, 3641-3657, doi:10.5194/acp-18-

755   3641-2018, 2018.

756

Figure captions

Figure 1. Representative mass spectrum for NOCs-containing particles. The ion

peaks corresponding to NOCs and oxidized organics are highlighted with red bars.

Figure 2. The variation in hourly mean Nfs of the oxidized organics and

ammonium that internally mixed with NOCs. Box and whisker plot shows lower,

median and upper lines, denoting the 25th, 50th and 75th percentiles, respectively; the

lower and upper edges denote the 10th and 90th percentiles, respectively.

Figure 3. Correlation analysis of (a, c) the RPAs and (b, d) the number of

detected NOCs, with the oxidized organics and ammonium in different seasons.

Significant ($p < 0.01$) correlations were obtained for both the total observed data and

the seasonally separated data. RPA is defined as the fractional peak area of each m/z

relative to the sum of peak areas in the mass spectrum and is applied to represent the

relative amount of a species on a particle (Jeong et al., 2011; Healy et al., 2013).

Figure 4. Comparison between the measured and predicted RPAs for NOCs.

Figure 5. (left) PMF-resolved 3-factor source profiles (percentage of total species)

and (right) their diurnal variation (arbitrary unit).

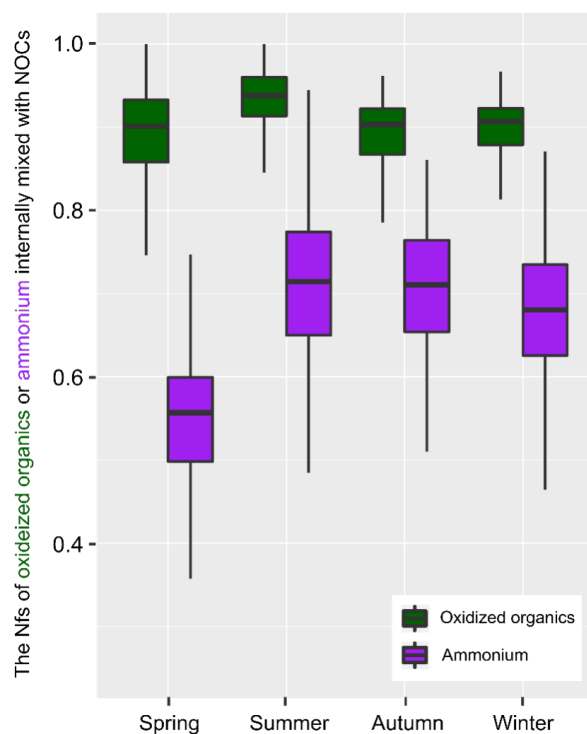Figure 6. The dependence of NOCs and the ratio of NOCs to the oxidized organics

on RH.

Figure 7. The dependence of NOCs on the relative acidity ratio. The relative

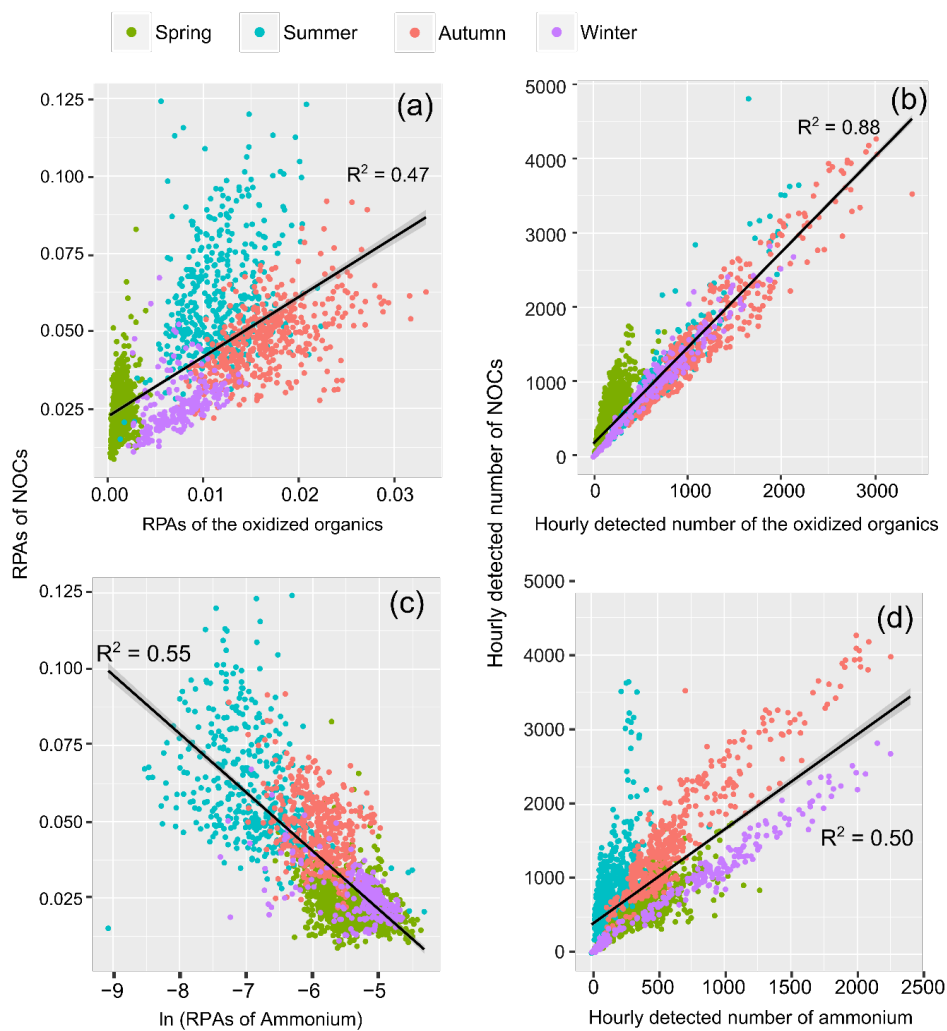acidity ratios were logarithmically transformed to follow a normal distribution.
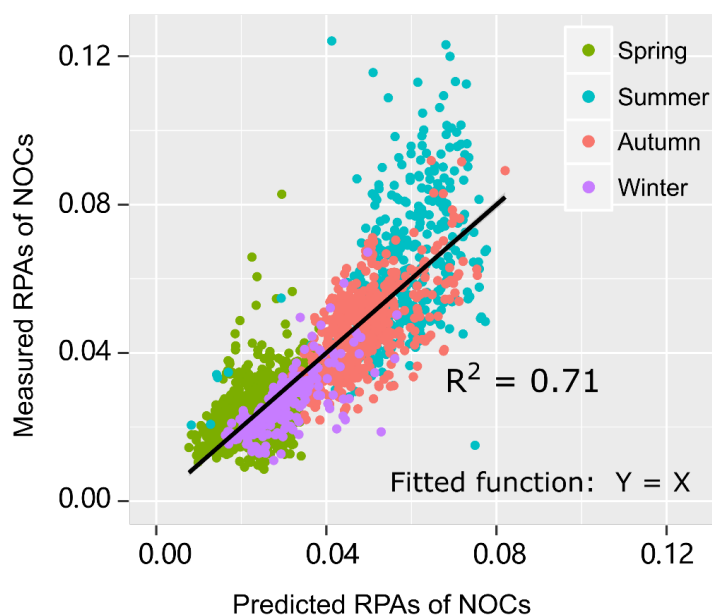
777

778   Fig. 1.

Atmospheric
Chemistry
and Physics
Discussions

Open Access

EGU

779

780   Fig. 2.

781

782   Fig. 3.

Atmospheric
Chemistry
and Physics
Discussions

783
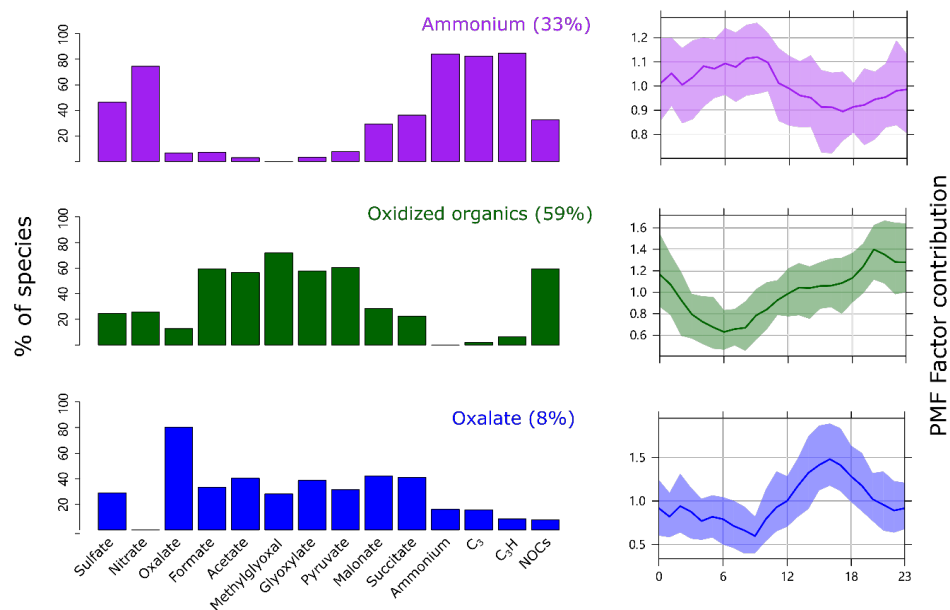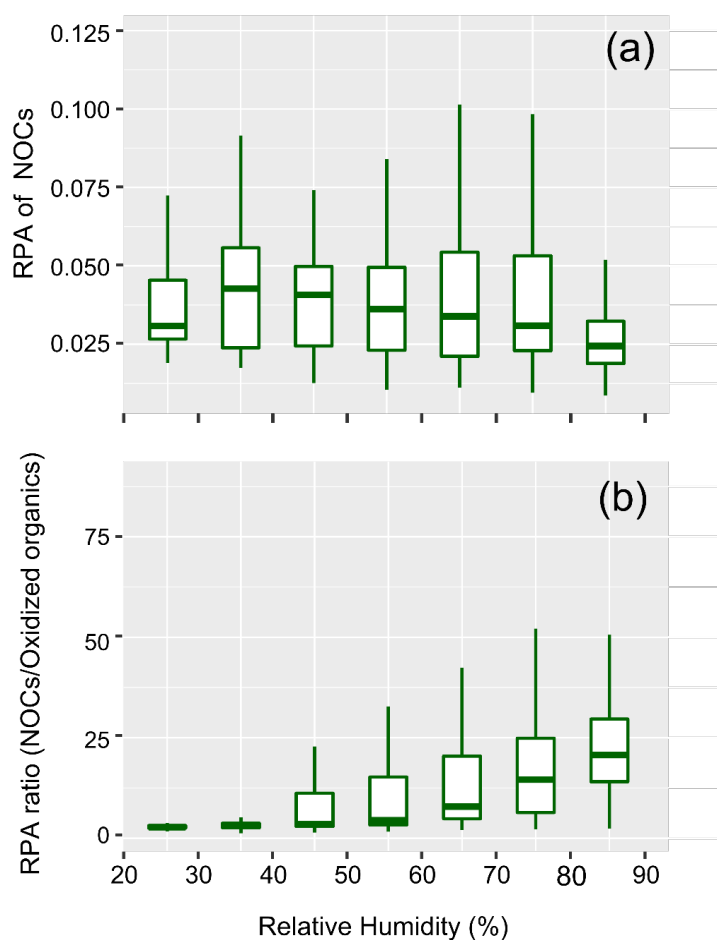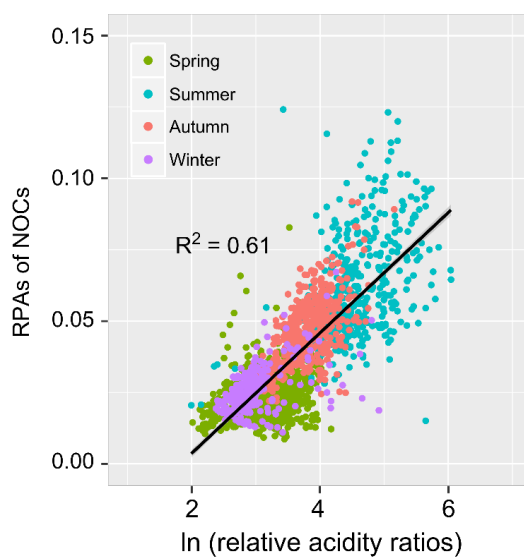
784   **Fig. 4.**

785

786

787   **Fig. 5.**

788

789   **Fig. 6.**

790

791   **Fig. 7.**